New procedures to evaluate the performance of protection barriers in rockfall risk assessment

A. Mentani[1)], D. Toe[2)]

[1)] **DICAM Alma Mater Studiorum Università di Bologna**
[2)] **Université Grenoble Alpes, Irstea, UR EMGR**

1 Introduction

In the existing rockfall risk assessment procedures the effectiveness of the installed protection structures, like barriers, to events predicted by rockfall trajectory tools is missing. This study proposed new methods to evaluate the performance of protection barriers with computational cost effective solutions. The rockfall barrier capacity is defined in terms of the maximum kinetic energy, possessed by the impacting body, the barrier is able to arrest. This capacity can be determined based on full-scale test described by the European guidelines ETAG 027 (EOTA 2013). However, when installed in site, the barrier can be subjected to impact conditions which differ from the ETAG test. Recently, numerical models of rockfall barriers were developed (Gentilini et al. 2013, Escallon et al. 2014, Mentani et al. 2016). They are able to analyse the structure response, but their high computational cost made impossible to couple the model with any rockfall trajectory tools. On the contrary, due to their mathematical structure, meta-models can be easily integrated with that models. The study addresses the response of a cable-net rockfall barrier whose presence is widespread within the Alpine arc (de Miranda et al. 2015). A FE model of the barrier was developed to investigate its response to realistic impact conditions. A meta-model was then created based on the simulation results. Finally, an alternative approach to further reduce the computational cost of each simulation, by using a different mesh technique, was also introduced.

2 Cable-net rockfall barrier

2.1 Barrier details

The studied barrier is typically installed as a series of structural modules of 3.2 m height and 5 m width, each divided by steel posts fixed at the base. The sample used for the study consisted of 3 functional modules (Fig. 1a). The interception

structure was made of 15 evenly spaced longitudinal cables of 12 mm diameter. The cables were free to slide through the internal posts (IPE 200), while were restrained to the external posts (IPE 300). The external posts were also connected to the ground by side cables of 18 mm diameter. A secondary hexagonal meshwork was also installed with the function to intercept the smaller impacting bodies.

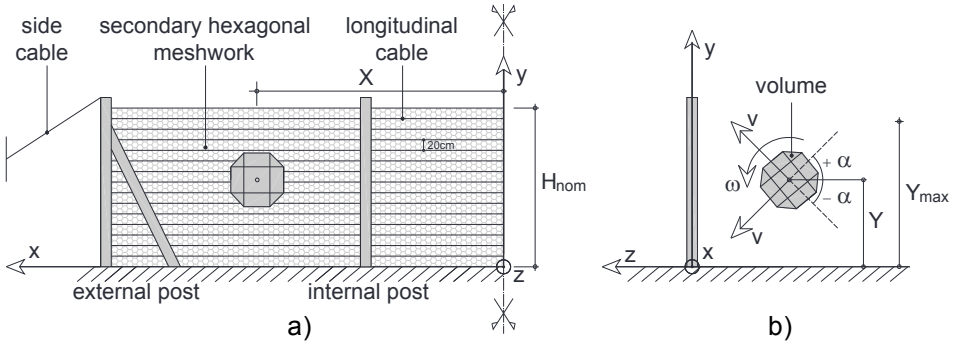

Fig. 1: Geometry of the cable-net protection barrier: a) front view and b) lateral view with input parameters for loading conditions.

2.2 FE model details

The model was built according to the barrier geometry using the commercial code Abaqus (Abaqus 2013). It is a 3D model made of one-dimensional elements, whose behaviour is governed by elasto-plastic constitutive laws. The posts were modelled with beam elements and behave an elasto-perfectly plastic law up to a failure limit, while truss elements obeying an elasto-plastic hardening law were used for the cables. The hexagonal wire mesh was modelled according to numerical choices defined by Mentani et al. (2016). Internal connections within barrier elements were managed with the use of connector elements between nodes, while a contact law using a Coulomb-friction model was assigned between the interception structure and the block (Toe et al. 2018).

3 Investigating the barrier performance

3.1 FE simulations

The barrier model was subjected to non-linear dynamic analyses in which a polyhedral block was impacting the structure with known mass and velocity. The explicit operator was used to the scope. In first place, a reference capacity of the barrier was estimated according to the standard defined by ETAG 027 (EOTA 2013). In the simulated test, a 640kg block impacted the central panel of the barrier with a translational velocity of 25 m/s, yielding a reference capacity of 200 kJ. The model was then used to investigate the influence of the loading conditions on the barrier performance. Among all, six input parameters, describing the block

incident trajectory for the wide variety of impact conditions, were considered: the block volume V; the translational and rotational velocity v and ω; the angle of incidence α; and the block impact position on the barrier X and Y (Fig. 1b). A plan of 300 simulations was established by varying the input parameters within a realistic range of values, deriving from what commonly encountered in rockfall trajectory simulation tools and field tests (Bourrier et al. 2009) and adapted to the barrier capacity. Parameters and ranges are listed in Table 1. The input parameters combinations were defined by using the Latin-Hypercube sampling method (Sacks et al. 1989) and a uniform distribution for each input parameters was considered.

Tab. 1: Input parameters for the loading conditions

Input parameter	**Unit**	**Range (min-max)**
Translational velocity, v	m/s	5 – 22.5
Rotational velocity, ω	rad/s	0 – 35
Volume of the block, V	m^3	0.03 – 2.5
Incident angle, α	deg	-60 – 60
Impact position, X	m	0 – 7.5
Impact position, Y	m	1 – 2.5

3.2 Analysis of the results

In Fig. 2a, each simulation result is reported as function of the block volume and translational velocity and the continuous line represents the barrier reference capacity (200 kJ). Triangles identified the 80 tests where the barrier was able to arrest the block (B_{succ}), while other symbols referred to failure events (B_{fail}). The barrier appeared inefficient for more than 30% of the cases below the reference limit curve. In particular, 3 different failure mechanisms were observed. One case did not concern failure of the structure, the block was impacting the barrier with an upward inclination and passed over the barrier by rolling out of the system (i.e. "rolling over"). The other two modes concerned failure of the structure. The first referred to perforation of the mesh: the block rolled through the cables and the secondary mesh was not able to arrest it. In the second case, a global failure mechanism of the barrier was observed, which was generally developed at the posts, due to formation of plastic hinges. Over the 220 barrier failures, in 80 cases the block rolled over the structure, 76 referred to mesh perforation and 74 to a global failure mechanism (Fig. 2a). The results suggested that the centred impact suggested by ETAG is far from being the most detrimental case to the barrier. Figure 2 also highlighted that investigating the barrier performance just considering the block volume and translational velocity doesn't allow a precise correlation with the expected failure mechanism.

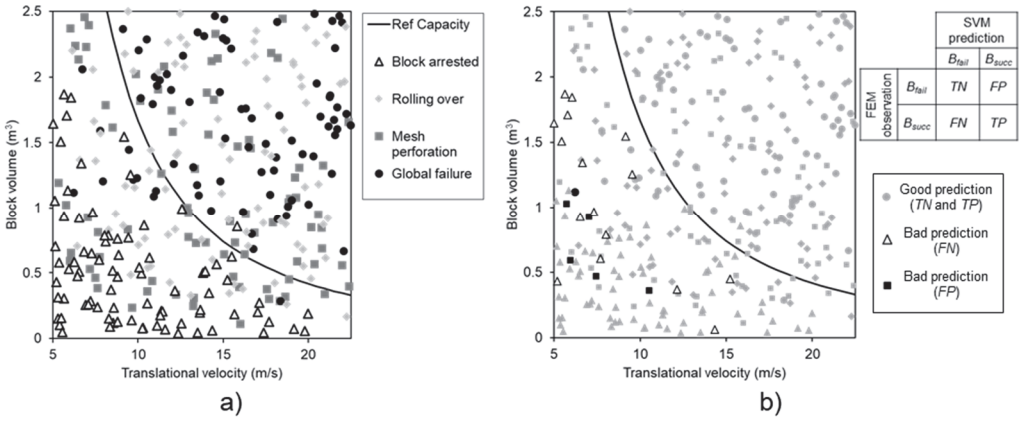

Fig. 2: Results of the simulations on the block velocity-volume plane: a) FE results with detection of barrier success (B_{succ}) or failure (B_{fail}) and b) prediction of the SVM meta-model.

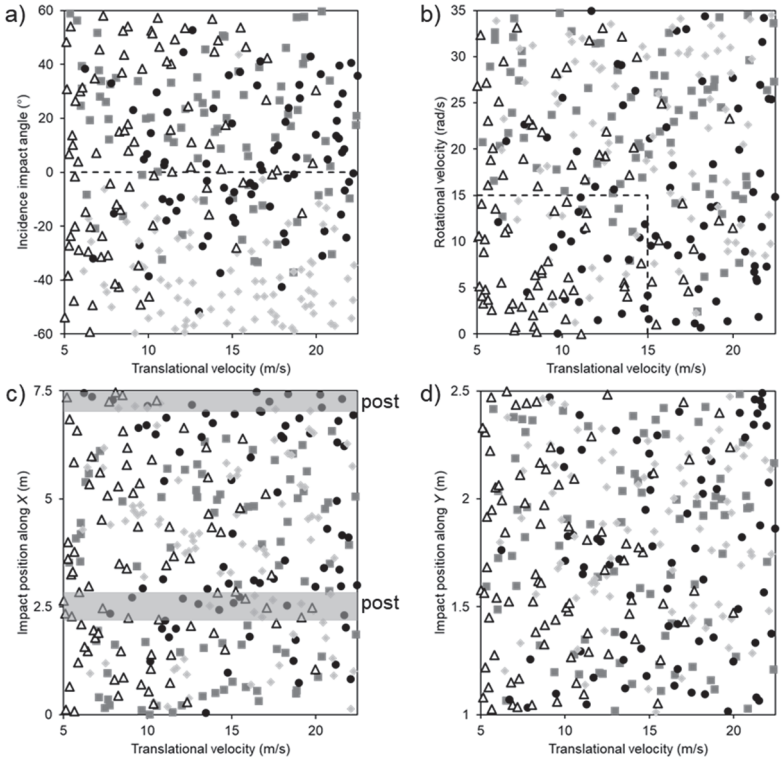

Fig. 3: Results of the simulations as function of block velocity and: a) incident angle; b) rotational velocity; c) and d) block position.

Some correlation can be identified by plotting the results in combination with the other 4 input parameters. Figure 3a shows that most of the rolling over cases concerned negative incidence angles at impact. The barrier capacity to arrest the block was reasonably decreasing with increasing rotational velocity and it can be observes that most of the mesh ruptures consisted of ω larger than 15 rad/s (Fig. 3b). If plotting the data as function of the block location at impact, no particular correlation between the failure mechanism and the y-position was observed (Fig. 3d), but global failure mostly occurred when the block impacted the barrier against or in the area close to the post (Fig. 3c). Figure 3 illustrates the weak points of the

given barrier considering the variety of impact conditions and may be used on design improvement purpose. However, the barrier response appeared extremely variable and its failure below the energetic reference capacity resulted from the activation of almost unpredictable mechanisms. This support the need for developing approaches that consider all the possible loading conditions.

3.3 The meta-modelling approach

Meta-models are mathematical operators defining relations between multiple input and output. Within the context of rockfall risk assessment, they can describe the response of a protection structure for a combination of input parameters, with particular aim on capturing the barrier capacity on arresting a block. To the scope, a Support Vector Machine (Brereton & Lloyd 2010) meta-model was used. A certain number of data is necessary to develop an optimised meta-model for a given structure, which is function of the numbers and variability of the input parameters. With reference to the studied rockfall barrier, the input/output data of the 300 numerical simulations were used.

3.3.1 The Support Vector Machine (SVM)

The Support Vector Machine (SVM) approach is based on statistical learning theory (Vapnik 1995) and can be used to predict the class of an output data. Two output were considered: the cases of barrier success (B_{succ}) or failure (B_{fail}). In the space of input parameters corresponding to the impact conditions, the SVM defines the optimal hyperplane separating the regions associated with the two classes. The hyperplane, called super vector, is built considering the closest points of the space and it is defined by maximising the distance between the plane and the closer points on each side. The construction of the SVM can require nonlinear transformation of the data to another space of potentially higher dimension using kernel functions (Baudat & Anouar 2001). The meta-model was thus created as a R function able to predict the barrier response (B_{succ} or B_{fail}) to any impact event.

3.3.2 Quantification of meta-model capacity

The n FEM simulation results $M(x_i)$ deriving from each parameters combination x_i were considered. The leave-one-out cross-validation method (Allen 1971) was used to analyse the SVM global accuracy $Q(M_{SVM})$. For each combination x_i a meta-model was created considering all the simulation outcomes except $M(x_i)$. The meta-model prediction $M_{SVM}(x_i)$ was then compared to $M(x_i)$. This process was applied to all the n combinations and the global accuracy was computed as:

$$Q(M_{SVM}) = 1 - \frac{1}{n}\sum_{i=1}^{n}\left[M\left(x_i\right) - M_{SVM}\left(x_i\right)\right] \quad (1)$$

The effectiveness of the SVM meta-model prediction was also analysed in terms of misclassification rates. For each test, the SVM can provide bad (false, *F*) or good predictions (true, *T*) with respect to the FE observations. In both cases the prediction can be either positive (*P*), if barrier success on arresting the block was estimated, or negative (*N*), when failure was evaluated. Four cases were thus identified to describe the SVM predictions, as reported in Fig. 2b. Based on these definitions, two indicators were used to discuss the performance of the meta-model: the false negative rate FN_r=FN/(FN+TP) and the false positive rate FP_r=FP/(FP+TN). Within this context, the false positive rate is the most relevant to deal with as it focuses on the most critical situation. Indeed, a high FP_r value is associated to an overestimation of the barrier capacity by the meta-model.

3.3.3 Meta-model accuracy

Results predicted by the SVM meta-model are illustrated in Fig. 2b. Note that, grey symbols represent the two cases of good predictions (*TN* and *TP*), while bad predictions are reported with black symbols. Over the 300 results considered in this study, the SVM global accuracy was computed equal to 93.3% according to eq. 1. The meta-model failed to predict 16 barrier success over the 80 FE observations (FN_r = 20%). Differently, a false positive rate equal to 2.7% was computed as the SVM failed to predict 6 barrier failure over the 220 cases, thus resulting in the meta-model overestimating the barrier capacity.

3.4 Discussion about the time cost

The meta-model represents an effective solution to investigate a rockfall barrier performance. However, the computational cost of the FE model should be considered when developing a SVM. All the simulations considered in the study were run using an Intel Xeon E3-1240 v5 processor at 3.50 GHz. The computation time of each simulation was highly variable and was influenced by many of the input parameters, but an average cost of about 90 min was necessary. This means that a total of 450 working hours were requested to develop the SVM meta-model.

4 An alternative approach to reduce the FE computational cost

4.1 The equivalent continuum approach

An alternative strategy to reduce the computational time of each simulation is proposed. The study considered a rockfall barrier whose interception structure was

made of a chain-link wire mesh manufactured by Geobrugg (Fig. 4). The proposed method analysed the opportunity to model the mesh via an equivalent continuum approach by using triangular finite-strain shell elements with reduced integration control. They are thin shell elements based on the Kirchoff-Love plate theory. The choice of adding a reduced integration control implies a lower-order of integration to form the element stiffness, thus decreasing the CPU time (Barlow 1976).

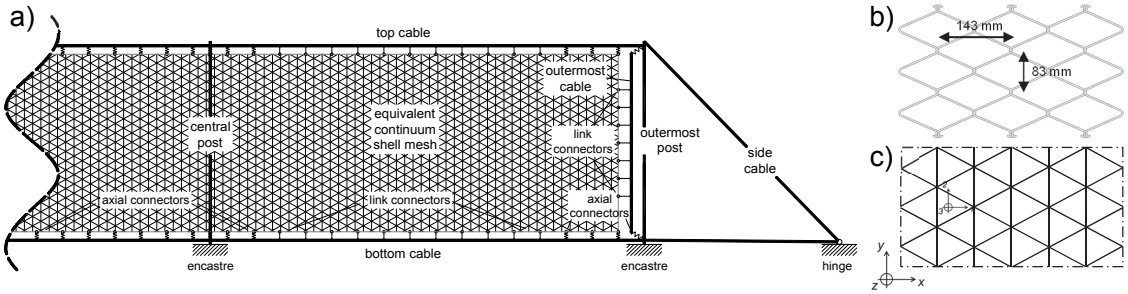

Fig. 4: a) Sketch of the rockfall protection barrier with: b) chain-link wire mesh and c) equivalent continuum mesh with triangular shell elements

As for the model constitutive law, plane stress conditions were considered for the shell elements. A linear elastic orthotropic behaviour was assigned to account for the anisotropic behaviour of the chain-link mesh. Thus, 4 elastic parameters defined the matrix stiffness: the Young moduli in the mesh plane (E_1 and E_2), the shear modulus (G_{12}) and the Poisson' coefficient (ν_{12}). The Hill criterion (Hill 1950) was used to define the mesh response in the plastic phase. The Hill's yield function is expressed by:

$$f(\sigma) \equiv \frac{1}{X^2}\sigma_{11}^2 - \left(\frac{1}{X^2} + \frac{1}{Y^2} - \frac{1}{Z^2}\right)\sigma_{11}\sigma_{22} + \frac{1}{Y^2}\sigma_{22}^2 = 1 \qquad (2)$$

where X, Y and Z are yield stress parameters governing the size of the yield surface. An associated flow rule is then considered to account for plastic strains. A ductile damage criterion was implemented to capture the mesh failure. It considers a limit value of the equivalent plastic strain ($PEEQ_f$) accumulated within each shell element of the mesh. Further details on the material properties adopted for the shell elements can be found in Mentani et al. (2018).

4.1.1 Calibration of the model parameters

The elastic properties were identified on the base of experimental tensile tests carried out on mesh portions in the two in-plane principal directions. Results of the two tests are reported in Fig. 5a in terms of forces and mesh elongation, showing the mesh anisotropy in the two principal directions. The plastic criterion was then calibrated based on impact tests carried out on a 2m side squared mesh. In the test a concrete block of 440 kg mass was released from 0.85m height to impact the central point of the wire mesh after free fall. The elastic model was not able to

capture the dissipation mechanism after the first peak and the introduction of plasticity was necessary to capture the block displacement with time (Fig. 5b). Another test, where the mesh failed to arrest the impacting block, was considered to estimate the failure parameter able to reproduce the result (Fig. 5c). Table 2 provides the calibrated values of the 8 model parameters of the equivalent model.

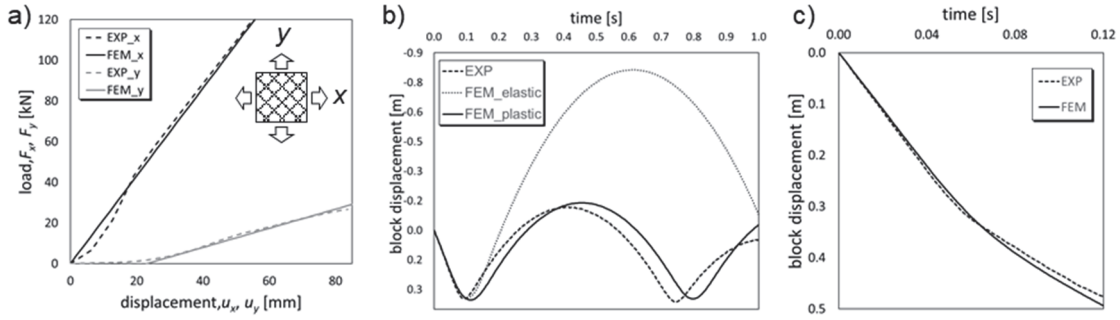

Fig. 5: Comparison of numerical and experimental results: a) tensile tests in *x* and *y* directions; b) and c) impact tests.

Tab. 2: Input parameters for loading conditions

Elastic domain				Plastic domain			Failure
E_1 (MPa)	E_2 (MPa)	G_{12} (MPa)	v_{12}	X (MPa)	Y (MPa)	Z (MPa)	$PEEQ_f$
630	90	9	0.3	25	10	10	0.35

4.2 Modelling a rockfall barrier with shell elements

The result of a full-scale test carried out on the barrier was considered to assess the adopted strategy. In the test, a block of 665kg impacted the barrier central panel with a velocity of 9.6m/s. The block was arrested and a maximum displacement of 1.74 m was measured. The FE model (Fig. 4) was built adopting the same numerical choices described in Section 2, but the interception structure was modelled with shell elements. A comparison of the experimental and numerical results is reported in Fig. 6.

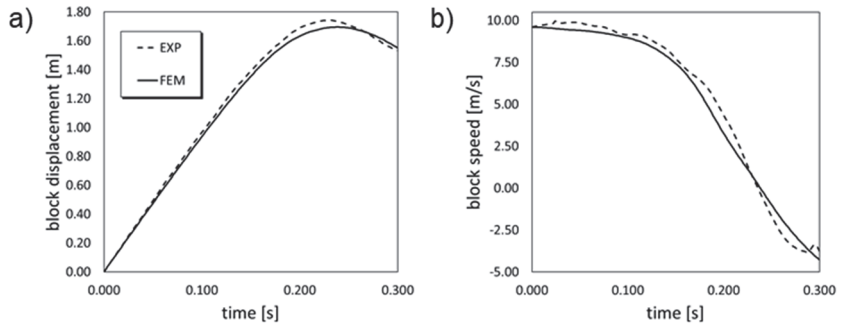

Fig. 6: Results of the experimental and numerical tests performed on the chain-link barrier.

The model proved its ability on reproducing the experiment, both in terms of maximum block displacement and velocity decay, thus validating the reliability of the equivalent continuum approach to reproduce the response of a rockfall barrier.

4.3 Model computational cost

The barrier test simulation was carried out with the same processor machine described in Section 3.4 and the required computation time was less than 5 min. This represents a great advance in the idea of using the equivalent model for a parametrical study of the barrier response. As an example, the SVM meta-model of the chain-link mesh barrier could be developed, by running the 300 simulations as in previous case, in a day time (25h).

5 Concluding remarks

In the proposed study, the performance of a rockfall barrier was first investigated by running parametric simulations with a FE model. The simulation results allowed to gain a detailed and global image of the barrier response for any realistic loading case. The numerical outcomes were then used to develop a meta-model able to predict the barrier response to any impact event. The meta-model represents a cost and time-effective solution if compared to full-scale tests to be performed on the barrier. It consists of a R function, representing the barrier behaviour, which can be easily coupled to any rockfall trajectory analysis tool. A consideration on the computational cost of the FEM simulation was also added and a novel approach to reduce the CPU time by using an equivalent continuum mesh technique was introduced. These approaches appear promising to assess the barrier efficiency and improve rockfall quantitative hazard assessment with cost effective solutions.

6 Literature

Abaqus (2013)
Abaqus analysis user manual. Version 6.11.

Allen, D.M. (1971)
The prediction sum of squares as a criterion for selecting predictor variables. University of Kentucky, Lexington

Barlow, J. (1976)
Optimal stress locations in finite element models. Int J Numer Meth Eng. Vol 10, 243-251.

Baudat, G. & Anouar, F. (2001)
Kernel-based methods and function approximation. Proc Int Jt Conf Neural Netw. Vol 2, 1244–1249.

Bourrier, F., Dorren, L., Nicot, F., Berger, F. & Darve, F. (2009)
Toward objective rockfall trajectory simulation using a stochastic impact model. Geomorphology. Vol 110, No. 3-4, 68-79.

Brereton, R.G. & Llyod G.R. (2010)
Support Vector Machines for classification and regression. Analyst. Vol 135, No. 2, 230-267.

de Miranda, S., Gentilini, C., Gottardi, G., Govoni, L., Mentani, A. & Ubertini, F. (2015)
Virtual testing of existing semi-rigid rockfall protection barriers. Eng Struct. Vol 85, 83-94.

Escallon, J.P., Wendeler, C., Chatzi, E. & Bartelt, P. (2014)
Parameter identification of rockfall protection barrier components through an inverse formulation. Eng Struct. Vol 77, 1-16.

EOTA (2013)
ETAG 027: guideline for European technical approval of falling rock protection kits.

Gentilini, C., Gottardi, G., Govoni, L., Mentani, A., & Ubertini, F. (2013)
Design of falling rock protection barriers using numerical models. Eng Struct. Vol 50, 96-106.

Hill, R. (1950)
The mathematical theory of plasticity. Clarendon press, Oxford.

Mentani, A., Giacomini, A., Buzzi, O., Govoni, L., Gottardi, G. & Fityus, S. (2016)
Numerical modelling of a low energy rockfall barrier: new insight into the bullet effect. Rock Mech Rock Eng. Vol 49, No. 4, 1247-1262.

Mentani, A., Govoni, L., Giacomini, A., Gottardi, G. & Buzzi, O. (2018)
An equivalent continuum approach to efficiently model the response of steel wire meshes to rockfall impacts. Rock Mech Rock Eng. Doi: 10.1007/s00603-018-1490-5

Sacks, J., Welch, W.J., Mitchell, T.J., Wynn, H.P. (1989)
Design and analysis of computer experiments. Stat Sci. Vol 4, No.4, 409-423

Toe, D., Mentani, A., Lambert, S., Govoni, L., Gottardi, G. & Bourrier, F. (2018)
Introducing meta-models for a more efficient hazard mitigation strategy with rockfall protection barriers. Rock Mech Rock Eng. Vol 51, No. 4, 1097-1109.

Vapnik, V. (1995)
The nature of statistical learning theory. Springer, Berlin.